

28 INTRODUCTION

29 Pipe-jacking may have become the preferred delivery method over conventional open
30 trenching for installation of buried infrastructure, largely due to the mitigated disturbances to
31 ground surface, as well as the reduced disruptions to road traffic. Such trenchless technology
32 methods involving micro-tunneling can be implemented in the form of pipe-jacking. Pipe-
33 jacking works in the central business district of Kuching City, Malaysia were necessary as
34 trunk sewer lines were proposed to be installed in depths up to 25 m from the existing ground
35 level. The pipe-jacking works traversed the pre-upper carboniferous Tuang Formation,
36 characterized by highly fractured and tightly folded phyllite, with highly fractured
37 lithological units of shale, metagreywacke, and sandstone (Tan, 1993). The relatively young
38 and weathered geological formation created challenges during extraction of rock cores in soil
39 investigation (SI) works, particularly from the argillaceous units of shale and phyllite. The SI
40 works revealed that majority of the recovered cores of shale and phyllite had a Rock Quality
41 Designation (RQD) value of zero. RQD is defined as the total length of recovered cores
42 longer than 100 mm expressed as a percentage of the total rock core length (Deere, 1989).
43 The low RQD values implied a lack of suitable core lengths for uniaxial compression strength
44 (UCS) and point load testing. This made it difficult to assess the in-situ weathered rock
45 strength parameters as the preferred in-situ pressuremeter tests were not readily available at
46 that point in time. Furthermore, local expertise in the industry in performing the in-situ
47 pressuremeter tests was very limited. Unfortunately, pressuremeter tests were not originally
48 budgeted for in the investigation stage of the project.

49 This study was motivated by the possibility of using tunneling rock spoils for the purpose
50 of back-analyzing pipe-jacking forces during the construction of trunk sewer lines in Kuching
51 City, Malaysia (Choo and Ong, 2012). Rock spoils from tunneling works were collected from
52 four different pipe-jacking drives. Direct shear testing of reconstituted tunneling rock spoils

53 was used as an alternative method of obtaining rock strength parameters so that pipe-jacking
54 forces could be reliably understood and back-analyzed. Results from direct shear tests were
55 applied to a well-established empirical pipe-jacking force equation. The calculated pipe-
56 jacking forces with respect to drive lengths were compared to corresponding measured values.
57 It has been found that the back-analyzed values of μ agreed reasonably well with the
58 suggested range of $\mu = 0.1\text{--}0.3$ considering lubrication (Stein et al., 1989) and must be
59 explained with reference to their surrounding geologies due to soil-structure interaction.

60 **DIRECT SHEAR TESTING**

61 The direct shear test has been used to determine shear strength properties of various soil-
62 structure interfaces. Such applications of direct shear testing range from fundamental studies
63 on the effects of dilatancy (Simoni and Houlsby, 2006), particle size (Yu et al., 2006) and
64 shear box platen fixities (Jewell, 1986) to field applications including skin friction generated
65 between various construction materials (Potyondy, 1961), geosynthetic-reinforced structures
66 (Anubhav and Basudhar, 2013; Arulrajah et al., 2013), large-scale hydropower projects, and
67 excavations of lunar regoliths (Iai and Luna, 2011). Direct shear tests can be conducted under
68 conditions of constant normal load (CNL), constant normal stiffness (CNS), or constant
69 volume (CV) (Pellet and Keshavarz, 2014). The direct shear tests in this current study were
70 conducted under CNL conditions to reflect the in-situ stress conditions along the drives.

71 The direct shear test has also been used for studies on pipe-jacking forces. The effect of
72 surface roughness for some common jacking pipe materials was studied by displacing the top
73 half of a shear box along the outer periphery of the studied pipes (Staheli, 2006). The shear
74 box was filled with sand and respective frictional coefficients for the respective pipe
75 materials were produced. The frictional coefficients were subsequently applied to back-
76 analyses of measured jacking forces from actual pipe-jacking drives. A frictional jacking

77 force model was developed from the back-analyses; however this force model was developed
78 for unlubricated drives traversing clays and sands only.

79 A separate study on the effect of lubrication using a modified shear box, involves the
80 dragging of a concrete block over a large sample of soil (Shou et al., 2010). Lubricant was
81 placed between the concrete block and the soil. Measurements were made of the critical drag
82 force required to move the concrete block, with variations made to the lubricant type and
83 applied normal force on the concrete block. An unlubricated condition was used as a
84 benchmark. The results showed that the lubricant mix of plasticizers with polymer fluid
85 reduced the pipe-soil interface friction by 75%, due to the discrete layer of plasticizer present
86 between the concrete block and soil. The findings were subsequently applied to a case study
87 of a 2.85 m diameter pipe of length 400 m jacked through gravel at a depth of 9.65 m below
88 the ground surface. There was a large discrepancy between the back-analyzed jacking forces
89 against those resulting from the modified direct shear test. This discrepancy was attributed to
90 the overestimation of the pipe-soil contact area.

91 Therefore, in view of limited studies on pipe-jacking in relatively young, weathered
92 sedimentary and metamorphic rocks, this paper makes a novel attempt to effectively quantify
93 jacking forces via a systematic approach of utilizing reconstituted rock spoils tested in a
94 direct shear apparatus.

95 **EMPIRICAL METHOD TO DETERMINE JACKING FORCES**

96 Some commonly used equations for predicting forces in pipe-jacking works through soil
97 have been derived statistically (Chapman and Ichioka, 1999), empirically (Osumi, 2000), or
98 experimentally (Staheli, 2006). Very limited considerations are made for drives in rock. In
99 empirically derived jacking force models, two approaches are used for assessing frictional
100 jacking forces.

101 The first considers the soil stresses acting on the outer periphery of the pipeline. This
 102 approach is typically dependent on the strength properties of the geology surrounding the
 103 pipe. However, the usage of such equations is often restricted to drives traversing sands or
 104 clays, with limited experience for tunneling through weathered rocks. The evaluation of
 105 jacking forces through weathered rocks can be made further complicated due to the
 106 surrounding highly fractured rock mass or, in contrast, the presence of an arching effect.

107 Pellet-Beaucour and Kastner (2002) developed a jacking force equation, which
 108 incorporated the geomechanical phenomenon of soil arching. Terzaghi (1936) observed this
 109 phenomenon through the introduction of a trap door beneath a sand mass. Opening the trap
 110 door disturbed the geostatic stresses, thus inducing a relaxation of soil stresses above the trap
 111 door. Such phenomenon is also evident in rock tunnels. Hence, the model developed by
 112 Pellet-Beaucour and Kastner (2002) was chosen for use in this paper due to its inclusion of
 113 the soil arching effect. This jacking force model is shown in Eq. (1), which is expressed as
 114 the vertical soil stress at the pipe crown, σ_{EV} shown in Eq. (2).

$$115 \quad F = \mu L D_e \frac{\pi}{2} \left[\left(\sigma_{EV} + \frac{\gamma D_e}{2} \right) + K_2 \left(\sigma_{EV} + \frac{\gamma D_e}{2} \right) \right] \quad (1)$$

$$116 \quad \sigma_{EV} = \frac{b \left(\gamma - \frac{2C}{b} \right)}{2K \tan \phi} \left(1 - e^{-2K \frac{h}{b} \tan \phi} \right) \quad (2)$$

117 where F = total frictional jacking force; L = pipe span; D_e = outer pipe diameter; γ = soil unit
 118 weight; h = soil cover from the ground level to the pipe crown; K = lateral earth pressure
 119 coefficient; K_2 = thrust coefficient of soil acting on the pipe, with a suggested value of 0.3
 120 (French Society for Trenchless Technology, 2006); C = soil cohesion; and ϕ = soil internal
 121 friction angle. C and ϕ are derived from the in-situ rock mass above the pipe, where arching
 122 would develop. b is the influencing soil width above the pipe and is expressed in Eq. (3) as

123
$$b = D_e \left(1 + 2 \tan \left(\frac{\pi}{4} - \frac{\varphi}{2} \right) \right) \quad (3)$$

124 The formulation of σ_{EV} is based on the classic limit equilibrium approach developed by
125 Terzaghi (1943), which was dependent on the Mohr-Coulomb (MC) strength parameters of
126 the yielding soil.

127 During pipe-jacking works, tunnel boring creates changes to the geostatic stresses,
128 resulting in soil relaxation around the tunnel and pipe. This phenomenon redistributes soil
129 stresses around the bored tunnel, allowing the tunnel to self-stand through the phenomenon of
130 arching. The result is a reduction of vertical stresses experienced at the pipe crown, σ_{EV} .

131 μ is the coefficient of pipe-soil friction, given in Eq. (4) as

132
$$\mu = \tan \delta \quad (4)$$

133 where δ = pipe-soil friction angle.

134 For Eq. (1), values of μ between 0.1 – 0.3 were recommended for lubricated drives or
135 ‘fluid friction’ (Stein et al., 1989). These values for lubricated drives were previously used
136 for the prediction of jacking forces during tunneling in sands and clays (French Society for
137 Trenchless Technology, 2006; Pellet-Beaucour and Kastner, 2002), as well as limestone
138 (Barla et al., 2006). Pellet-Beaucour and Kastner (2002) reported μ values below 0.1, which
139 also indicated adequate lubrication. The recommended frictional coefficients for lubricated
140 drives assume ideal lubricating conditions, whereby a distinct lubricating layer is formed
141 between the jacked pipeline and the surrounding geology.

142 The use of these jacking force models is still dependent on the surrounding rock strength
143 characteristics and pipe-rock interface properties, which are difficult to assess in this Kuching
144 City study due to the friability of the extracted rock cores from the Tuang Formation. A novel
145 approach of acquiring the representative rock strength properties from reconstituted tunneling
146 rock spoils for the assessment of jacking forces is thus studied hereinafter.

147 **PROPOSED METHOD OF TESTING RECONSTITUTING ROCK SPOILS**

148 Rock cores obtained from the SI works at the launching and retrieving shaft locations
149 along the Tuang Formation in Kuching City revealed very low RQD values. The average
150 RQD value was 17% for rock cores obtained from the studied drives. In total, 30.7 m of core
151 lengths were extracted, of which 13.4 m produced RQD values of zero. A majority of these
152 extracted cores were highly fractured and not fully intact.

153 Similar observations were made by Ong and Choo (2011) for a separate project sited also
154 in the Tuang Formation. In this case study, 206 m of rock cores were extracted, of which 151
155 m had RQD values of zero. This provided challenges in conducting UCS tests and
156 consequently difficulties in obtaining useful, consistent strength values.

157 In other microtunneling projects, it may have been possible to survey the rock faces
158 exposed in more detail during shaft construction (Barla et al., 2006). In this study,
159 unfortunately exposed rock faces were quickly shotcreted as stand-up time was critical to
160 prevent water ingress, which would have resulted in ground surface deformations. Therefore,
161 joint directions of the rocks could not be further studied.

162 Furthermore, tests for determining strength anisotropy (e.g. UCS, Brazilian tensile test,
163 triaxial test, point load test, shear wave velocity) are usually conducted on intact cylindrical
164 cores (Bhasin et al., 1995; Desai and Salami, 1987; Gurocak et al., 2012; Saroglou et al.,
165 2004; Shea Jr and Kronenberg, 1993; Yilmaz, 2009) or prismatic specimens (Ramamurthy et
166 al., 1993; Singh et al., 2002; Tiwari and Rao, 2007). As a result of the challenges in obtaining
167 natural intact rock cores of suitable lengths, and also due to the friability of the in-situ rock, it
168 was not practically possible to ascertain the anisotropy of the rock mass.

169 Thus, a novel method to test and assess the reconstituted micro-tunneling rock spoils was
170 initially developed for a typical pipe-jacking drive in Kuching, Malaysia (Choo and Ong,
171 2012). Literature review shows that the reconstitution of rock fragments has been

172 successfully conducted on Australian black coal in order to homogenize the high variability
173 of its mechanical properties (Jasinge et al., 2009). Cement was used to stabilize the coal
174 samples. UCS and PLT tests were conducted on the reconstituted stabilized coal. The testing
175 results indicated reasonable homogeneity of the strength of the reconstituted coal. This
176 particular study successfully showed good potential in obtaining useful strength parameters
177 and correlations for reconstituted rock samples. This fundamental understanding was applied
178 hereinafter to allow for direct shear testing of tunneling rock spoils to obtain the relevant
179 shear strength properties.

180 In the current study, as the in-situ rock mass is naturally friable due to deep weathering in
181 a hot and humid climate (Malaysia is located on the Equator) (Tan, 1993), the concept of
182 reconstituting the excavated spoils into a shear box is to ‘re-create’ the situation of intensely
183 fractured, irregular and poorly sorted rocks with many arbitrary joints or fine cracks found on
184 the surfaces of the in-situ samples. This could be described as a highly weathered ‘soft rock’
185 which perhaps behaves more closely to soil, and hence the possible use of ‘soil’ equations as
186 shown in Eqs. (1) and (2). If proven reliable, research into the properties of reconstituted
187 tunneling rock spoils could provide a platform for consistent prediction of jacking forces
188 accrued during pipe-jacking works in highly fractured geology.

189 **Characteristics of test samples**

190 Petrographic analyses of thin sections were conducted on rock cores obtained from pipe-
191 jacking shaft locations. Fine-grained sandstone (metagreywacke) (see Fig. S1(a)) was
192 composed mainly of angular to subangular quartz grains. X-ray diffraction (XRD) tests
193 conducted on the samples of sandstone further validated the presence of quartz. Grains of
194 shale were mainly composed of clay minerals and silt-sized quartz grains, with tiny flakes of
195 mica (see Fig. S1(b)). Metamorphic phyllite was mainly composed of fine-grained quartz
196 with flaky sericite and mica (see Fig. S1(c)). The grains in phyllite were finer than those

197 found in shale. XRD tests did not reveal the presence of bentonite slurry, if any. (Note that
198 petrographic images can be found in Fig. S1 in the Supplemental Data.)

199 Test samples of tunneling rock spoils were obtained from desanding machines or
200 decantation chambers at four pipe-jacking sites in Kuching, Malaysia. Samples were
201 collected from the decantation chambers, which removed coarse particles from the tunneling
202 rock spoils transported from underground up to the ground surface by a slurry system. The
203 decantation chambers used standard screens mounted on shaker decks to segregate coarser
204 spoils from the transport slurry thus allowing for reuse of the slurry fluid for continued
205 transportation of tunneling rock spoils.

206 The particle size distribution tests of the tunneling rock spoils were conducted according
207 to testing standard ASTM D422-63 (2002). The particle size distribution curves for the
208 tunneling rock spoils before and after scalping are presented in Fig. 1. Scalping was
209 conducted to fulfil direct shear test requirements. Based on sieve analysis, both sets of spoils
210 (before and after scalping) comprised of sand-sized grains and can be classified as poorly
211 graded tunneling rock spoils according to both the Unified Soil Classification System (ASTM,
212 2000) and the Australian Soil Classification System (Standards Australia, 1993). Table 1
213 shows the results of sieve analyses performed on the scalped spoils.

214 **EXPERIMENTAL PROCEDURE**

215 Strain-controlled drained direct shear tests were conducted on the tunneling rock spoils in
216 accordance to ASTM D 3080 (2003) and AS 1289.6.2.2 (1998), through the use of the
217 GeoComp ShearTrac II apparatus. The fully automated direct shear system allows for full
218 automation of testing and extraction of test results, ensuring reliability of the tests. Control of
219 the testing parameters (consolidation, normal pressure, shear strain rate, and limits) was
220 achieved through pre-set limits of the automation functions, allowing for close scrutiny of
221 shear stresses and vertical displacements with horizontal deformation. The direct shear tests

222 were conducted under constant normal load (CNL) conditions to reflect the in-situ stress
223 conditions along the drives.

224 Scalping of the spoils was carried out in relation to the size of the shear box, where the
225 maximum particle size in the tested samples did not exceed 1/10th of the thickness of the test
226 specimen (Head, 1992). Successfully scalped samples were compacted in three layers within
227 the shear box by using a tamping plate to ensure even distribution of the compaction effort.
228 Test samples achieved relative densities ranging from 65% to 99% (see Table 1). Initial tests
229 were conducted at effective normal stresses representative of the in-situ overburden pressures
230 of the pipe-jacking works. Additional tests were performed beyond the confining pressures in
231 order to generate more data points to establish failure criteria. The said effective normal
232 stresses experienced by each sample type are also presented in Table 1. Specimens were
233 saturated and consolidated under the applied effective normal stresses until the completion of
234 primary consolidation, which was typically achieved within 5 minutes. ASTM (2003)
235 recommends for clean dense sands to be sheared at a rate computed from Eq. (6).

$$236 \quad d_r = d_f / t_f \quad (6)$$

237 where d_f = estimated horizontal displacement rate at failure (5 mm); t_f = total estimate
238 elapsed time to failure (600 sec for clean dense sands); and d_r = displacement rate (mm/sec).
239 Based on the recommended values for d_f and t_f , the shearing rate, d_r was 0.0083 mm/sec. A
240 lower shearing rate of 0.0017 mm/sec was adopted for dissipation of excess pore pressures, if
241 any. The samples were all tested to a maximum applied horizontal deformation of 15 mm,
242 which was sufficient to achieve residual state for the samples tested.

243 **DIRECT SHEAR TEST RESULTS**

244 The variations of shear stress and vertical displacements against horizontal displacement
245 from direct shear testing on scalped tunneling rock spoils are shown in Fig. 2(a). Test 1
246 showed distinct peak shear stress values for sandstone, before decreasing to a lower residual

247 shear stress value. For Tests 2, 3 & 4 on rock spoils of an argillaceous nature, the degree of
248 post-peak strain-softening was not as noticeable as tests conducted on rock spoils of an
249 arenaceous nature, i.e. sandstone. This was especially apparent on spoils of sedimentary shale.
250 Relatively large displacements were necessary to reach residual shear stresses, which is
251 typical of argillaceous materials. This was attributed to the larger grain sizes found in the
252 argillaceous spoils (Cerato and Lutenecker, 2006).

253 For vertical deformation (see Fig. 2(b)), positive values indicated compression of the test
254 specimen, while negative values indicated dilation. All tested samples showed initial
255 contractive behavior during initial increase of shear strain, indicating particulate interlocking.
256 In general, dilative behavior was observed upon reaching peak shear stresses. In Tests 2, 3 &
257 4, subsequent contraction was observed at relatively larger horizontal displacements in excess
258 of 8 mm, with larger applied effective normal stresses resulting in larger contractions.
259 Particle breakage appears to have occurred at this stage. This has been attributed to the flaky
260 and angular particles of shale spoils and phyllite spoils.

261 Non-linear strength envelopes for arenaceous (i.e. sandstone) and argillaceous (i.e. phyllite
262 and shale) rock spoils respectively are presented in Fig. 2(c). MC strength criteria were
263 initially developed based on regressive lines through the data points obtained from direct
264 shear testing. This was utilized to illustrate the shear strengths of the tested tunneling rock
265 spoils. However, the suitability of linear lines of best fit was dependent on the range of
266 stresses at which the specimens are tested. If not selected accurately, this may result in over-
267 estimation of shear strengths at extremely low or high stresses, while under-estimating shear
268 strengths at intermediate stress levels. Therefore, power law functions were considered.
269 Power law functions for geomaterials have been studied for various geotechnical applications
270 (Anyaeibunam, 2015; Lade, 2010; Soon and Drescher, 2007). De Mello (1977) introduced a
271 simplified power-type function stated as

272 $\tau = A \cdot (\sigma')^B$ (7)

273 where A and B are constants. This function was adopted by Charles and Watts (1980) and De
274 Mello (1977) in characterizing the non-linear shear strength behavior of rockfills. Table 2
275 lists the values of A and B based on test data from the tunneling rock spoils, using Eq. (7).
276 Values of B were typically between 0.6 and 1.0, which conform to power law exponent
277 values reported by Anyaegbunam (2015), i.e. $0 < B < 1$. For Test 2, a linear line of best fit
278 was sufficient to represent the data points. For convenience, the linear envelope was directly
279 characterized with a suitable MC criterion.

280 Despite the non-linearity of shear strength for the tested tunneling rock spoils, the jacking
281 force predictive model (Eqs. (1) & (2)) is dependent on the linear MC failure criteria, and
282 requires the use of values for c' & ϕ' . Yang and Yin (2004) introduced a “generalized
283 tangential” technique to approximate the non-linear power law failure criterion. Similar
284 approaches have been used in other applications (Collins et al., 1988; Drescher and
285 Christopoulos, 1988; Soon and Drescher, 2007). The non-linearity is simplified as linear MC
286 failure criterion tangential to the non-linear power law functions. Tangents to the respective
287 power-type curves were applied at the effective confining pressures pertaining to the
288 respective pipe-jacking depths (Fig. 2). Values for these tangential MC parameters for both
289 peak and residual phases are presented in Table 3. (Note that the direct shear test results and
290 interpreted strength profiles for Tests 2, 3, and 4 can be found in Fig. S2, Fig. S3, and Fig. S4
291 respectively in the Supplemental Data).

292 The tested specimens exhibited reduction in shear strength from peak to residual phases.
293 This was illustrated in the power function parameters by a decrease in A values, and a
294 corresponding increase in values of B (implying reduced curvature of the non-linear power
295 function). From the interpreted tangential MC parameters, drops in c' and ϕ' were also
296 observed. Generally, values of residual friction angle were lower than values corresponding

297 with peak frictional angle. Tested spoils of sandstone (Test 1) showed significant loss of
298 cohesion. Post-peak behavior of the sample suggests the formation of the shear zone, marked
299 by strain softening and dilation of the specimen. Li and Aydin (2010) attributed this to the
300 rotation and rolling of large particles, or larger quartz crystals (see Fig. S1(a)) as in the case
301 of Test 1.

302 In sands and gravels, friction angle ϕ' values decreased with increasing values of
303 coefficient of uniformity, C_u for frictional MC specimens (Wang et al., 2013). As stated
304 earlier, B indicates the curvature of the power function strength envelope. For peak shear
305 strengths, an increase in C_u from Test 1 to Tests 3 & 4 saw a decrease in the curvature of the
306 power function strength envelopes, as indicated by an increase in B . Hence, as C_u increased,
307 the variation of ϕ' with effective normal stresses was less apparent.

308 Spoils of shale (Tests 2 & 4) exhibited relatively low values of apparent cohesion. Peak
309 phases were not as apparent as those observed in Test 1, shown by the relatively minimal
310 dilation. Similar observations were made for phyllite spoils (Test 3). Phyllite spoils exhibited
311 the highest values for apparent cohesion, with only a slight decrease in cohesion from peak to
312 residual phases. In contrast to the blocky quartz crystals found in sandstone (Test 1), angular
313 and plate-like mica present in phyllite imply that formation of the shear zone was more likely
314 to be achieved through particle breakage than through rotation and rolling of the particles
315 (Lade et al., 1996).

316 **APPLICATION OF DIRECT SHEAR TEST RESULTS TO THE BACK-ANALYSIS** 317 **OF μ_{avg}**

318 Field measurements of pipe-jacking activities comprising of jacking forces, jacking speeds,
319 and lubrication use are shown in Fig. 3 for Drive A where tunneling rock spoils were
320 collected for direct shear testing. The interpreted geology, cumulative days elapsed, and
321 cumulative lubricant injected have also been included for the respective drives. (Note that the

322 field measurements of pipe-jacking activities for Drives B, C, and D can be found in Fig. S5,
323 Fig. S6, and Fig. S7 respectively in the Supplemental Data).

324 The jacking forces for the four pipe-jacking drives consisting of different geological
325 settings were studied. These jacking forces, with respect to the jacking length, were
326 characterized as gradients (kN/m), representing the average jacking forces for each drive,
327 respectively.

328 The strength parameters obtained from direct shear testing of scalped tunneling rock spoils
329 were used for back-analyses of the average jacking forces through the use of the jacking force
330 equations (Eqs. (1) & (2)). For calculation of vertical normal stress acting on the pipeline due
331 to arching, σ_{EV} (Eq. (2)), peak strength parameters c'_p & ϕ'_p were used in place of C & ϕ ,
332 respectively. Arching is caused by initial vertical slippage of the overburden soil or rock mass
333 over an excavated void during pipe-jacking. This usually occurs at low displacements of the
334 soil or rock mass into the bored tunnel. Hence, peak values were used for estimating σ_{EV} . In
335 some cases, the calculated σ_{EV} resulted in negative values, which implied tensile soil stresses
336 acting on the pipe. Terzaghi (1943) stated that beyond certain tunnel depths, the vertical
337 stresses at a tunnel roof were equal to zero. From Eq. (2), σ_{EV} is equal to zero provided

$$338 \quad b \leq \frac{2C}{\gamma} \quad (8)$$

339 Further explanation on the measured jacking forces shall be described in detail hereinafter.

340 **CASE STUDIES**

341 The case studies described hereinafter will illustrate the use of direct shear test results
342 from shearing of reconstituted tunneling rock spoils, back-analyzed frictional coefficients,
343 and effect of construction activities. The measured jacking forces are shown, superimposed
344 with calculated average jacking force profiles based on theoretical upper $\mu = 0.3$ and lower μ
345 $= 0.1$ bounds due to lubrication (Stein et al., 1989), and corresponding back-analyzed μ_{avg}

346 based on Eqs. (1) & (2) using measured jacking forces from Fig. 3. The respective values of
347 μ_{avg} have been compared against recommended frictional coefficient values of between 0.1
348 and 0.3 for lubricated drives, or ‘fluid friction’ (Stein et al., 1989). Table 4 shows the
349 measured pipe-jacking activities from the studied drives, including face support pressure,
350 pipe weight, TBM weight, jacking speed, and lubricant usage. The results from the back-
351 analyses of jacking forces based on results from direct shear tests are also presented.

352 **Drive A**

353 Fig. 3 shows jacking forces, jacking speeds and lubrication for Drive A which traversed
354 sandstone. The 1.43 m outer diameter, concrete pipeline (consisting of pre-cast, 3 m length
355 concrete pipes) spanned 140 m at a depth of 12.5m. The average volume of injected
356 lubrication was 47 L/m (see Fig. 3), into a theoretical overcut annulus of 87 L/m (see Table
357 4). This overcut region allowed for the injection of lubrication between the pipeline and the
358 surrounding geology. Extracted sandstone cores from the receiving shaft of Drive A had
359 majority RQD values of zero. The measured face support pressure was stable at 104 kN/m².
360 Hence, the measured jacking forces could be analyzed in terms of frictional resistance,
361 segregated from the face pressures. The jacking forces were well-represented with an average
362 line of best fit ($R^2 = 0.93$) at 14.4 kN/m (see Fig. 3). From direct shear testing of sandstone
363 (Test 1), the MC parameters for use in Eq. (2) were $C = c'_p = 50.8$ kPa and $\phi = \phi'_p = 47.8^\circ$
364 (see Fig. 2(c)). As stated previously, these values from the linear MC criterion were obtained
365 by utilizing the “generalized tangential” technique on the non-linear power law function. The
366 tangent to the non-linear function was applied at the effective overburden pressure with
367 reference to the tunnel depth. This resulted in $\sigma_{EV} = -20.8$ kN/m², indicating a significant
368 degree of arching over the pipe crown. However, negative values of σ_{EV} implied tensile
369 stresses acting normal to the outer pipe peripheral. For the back-analysis of μ_{avg} (see Eq. (1)),
370 σ_{EV} was adjusted to be equal to zero (Terzaghi, 1943). Fig. 4 shows the jacking forces

371 incurred during jacking through sandstone (Test 1), with the back-analyzed frictional
372 coefficient, $\mu_{avg} = 0.31$. Jacking force profiles corresponding with the recommended upper μ
373 $= 0.3$ and lower $\mu = 0.1$ limits of μ values for lubricated drives are also shown in Fig. 4. The
374 back-analyzed μ_{avg} of 0.31 matched with the upper limit of $\mu = 0.3$, as recommended by Stein
375 et al. (1989) for lubricated drives. This indicates that Drive A in sandstone was lubricated
376 moderately, confirmed by the comparison between injected volumes of lubrication and
377 theoretical overcut (see Table 4).

378 **Drive B**

379 Fig. S5 shows the jacking activities for Drive B. Similar to Drive A, the jacked pipeline
380 was of 1.43 m outer diameter. It also spanned 140 m at a depth of 12.5m. However, Drive B
381 negotiated through shale (Test 2). The volume of injected lubricant averaged 682 L/m (see
382 Fig. S5) and was significantly in excess of the theoretical overcut annulus of 87 L/m (see
383 Table 4). As summarized in Table 4, the extracted shale cores from the borehole done at both
384 receiving and jacking shafts had RQD values ranging from 0 to 80%, with a mean RQD of
385 26.0%. From Test 2, the equivalent tangential peak MC parameters were $c'_p = 0$ and $\phi'_p =$
386 41.4° (see Fig. S2). Using these values with Eq. (2), the calculated σ_{EV} was 34.1 kN/m^2 ,
387 indicating a reduced arching effect as compared to Drive A. The measured face support
388 pressure was constant throughout the drive at 68 kN/m^2 ; with the average jacking force
389 measured at 29.0 kN/m ($R^2 = 0.90$; see Fig. S8 of the Supplemental Data). The back-analyzed
390 frictional coefficient, μ_{avg} was 0.20. Fig. S8 illustrates that the back-analyzed μ_{avg} of 0.20 was
391 within the margin recommended by Stein et al. (1989) for lubricated drives, suggesting that
392 Drive B through shale was well-lubricated.

393 **Drive C**

394 Fig. S6 shows jacking activities for Drive C, which spanned 120 m through phyllite (Test
395 3). Tan (1993) reported phyllite from the Tuang Formation as being bedded, tightly folded
396 and highly sheared. From Table 4, it is observed that the extracted cores were characterized
397 by average RQD values of 17.5%, with 7.6 m of the total 15.1 m in extracted cores exhibiting
398 RQD values of zero. The average volume of lubricant injected was 181 L/m (see Fig. S6),
399 slightly in excess of the theoretical overcut of 113 L/m (see Table 4). From Test 3, the
400 tangential peak MC parameters were $c'_p = 57.8$ kPa and $\phi'_p = 44.3^\circ$ at $\sigma' = 222$ kPa (see Fig.
401 S3). Using these values with Eq. (2), the calculated σ_{EV} was -22.3 kN/m², demonstrating that
402 significant arching was present during pipe-jacking works at Drive C. The measured face
403 support pressure was stable at 47 kN/m². The average measured jacking force of 4.8 kN/m
404 ($R^2 = 0.78$) was the lowest of the jacking forces observed in this study (see Fig. S9 of the
405 Supplemental Data), with back-analyzed μ_{avg} of 0.07 , indicating that Drive C in phyllite was
406 very well-lubricated.

407 **Drive D**

408 Fig. S7 shows jacking forces for Drive D, a pipe-jacking drive spanning 228 m, which
409 navigated an initial 135 m section of stiff clay (SPT N value of 31), followed by a latter
410 section through shale (Test 4). Extracted shale cores from the borehole done at the receiving
411 shaft, corresponded with RQD values ranging from 10% to 23% with an average of 14% as
412 shown in Table 4. In the shale section of Drive D, an average of 729 L/m of lubricant was
413 injected into a theoretical overcut of 113 L/m (see Table 4). Tunneling shale spoils were
414 obtained from the latter section of the drive (136 m to 228 m) for direct shear testing (Test 4).
415 The equivalent tangential peak MC parameters were $c'_p = 29.0$ kPa and $\phi'_p = 38.7^\circ$ at $\sigma' =$
416 234 kPa (see Fig. S4). From Eq. (2), the computed σ_{EV} was 11.7 kN/m². The average face
417 support pressure had minimal fluctuations, measured at 115 kN/m². However, the measured

418 jacking forces were highly scattered ($R^2 = 0.45$) averaging at 81.1 kN/m (see Fig. S10 of the
419 Supplemental Data). This is believed to be due to a 19-day extended stoppage in the pipe-
420 jacking works, which occurred at the clay-shale interface (see Fig. S7). The subsequent back-
421 analyzed μ_{avg} was 0.71, indicating that lubrication during pipe-jacking of Drive D was
422 ineffective, despite having about 6.5 times more lubricant injected into the theoretical overcut.
423 This shall be explained in the discussion section later.

424 **Summary of drives**

425 Using the “generalized tangential” technique, equivalent MC parameters were estimated
426 from non-linear failure envelopes of direct shear tests on scalped tunneling rock spoils. These
427 tangential MC parameters have been used for the back-analysis of average measured pipe-
428 jacking forces through highly fractured rock formations of varying geology. Values of σ_{EV}
429 were computed based on Eq. (2) to provide indication of the arching effect in the studied
430 drives. The back-analyzed μ_{avg} values have been compared against μ values recommended by
431 Stein et al. (1989) for lubricated drives. The μ_{avg} values showed that the pipe-jacking drives
432 were lubricated, with the exception of Drive D which was affected by stoppages. These back-
433 analyzed μ_{avg} values were verified by the volume of injected lubrication. The effects of
434 arching, lubrication and stoppages shall be discussed hereinafter.

435 **DISCUSSION**

436 **Effect of arching on jacking forces**

437 In Drive A (sandstone), the calculated σ_{EV} value of -20.8 kN/m^2 was much lower
438 (representing relatively more arching effect) than that determined for Drive B (shale) at 34.1
439 kN/m^2 , resulting in approximately two times lower jacking forces for Drive A. Jacking
440 speeds were slightly higher in Drive A than in Drive B. In Drive A, the average injected
441 lubricant was 47 L/m or average 6,580 L for the entire length of 140 m, which was only a

442 fraction of the theoretical overcut volume of 12,180 L for 140 m. This may have explained
443 the back-analyzed μ_{avg} of 0.31, which is close to the 0.3 upper limit suggested for lubricated
444 drives by Stein et al. (1989).

445 The volume of lubricant injected for Drive B was 682 L/m, which was significantly in
446 excess of the theoretical overcut volume. The large volume of lubricant was injected as a
447 response to mitigate excessive increase in jacking forces. Back-analysis of the subsequent
448 jacking forces resulted in μ_{avg} of 0.20, which corresponds with the margin of 0.1 to 0.3
449 recommended for well-lubricated pipe-jacking drives by Stein et al. (1989).

450 The effect of geology on jacking forces, and consequently on jacking speed and lubricant
451 use was also apparent in Drive C (Test 3) through phyllite (see Fig. S6). The stress reduction
452 at the pipe crown due to presence of arching ($\sigma_{EV} = -22.3$ kN/m²) could also be attributed to
453 phyllite, which is characterized as being intensely folded with steep dips (Tan, 1993). Folds
454 were also depicted in micrographs of phyllite (see Fig. S1(c)). These geological features
455 created a structurally stable bore, allowing for re-distribution of soil stresses around the outer
456 peripheral of the pipeline, i.e. arching.

457 The erratic structure of phyllite also reduced the lubrication injected, as the intense folding
458 likely reduced the permeation of lubricant into the surrounding geology. The retention of
459 lubrication in the overcut ensured that the discretization of a lubricating layer was maintained.
460 This phenomenon has allowed Drive C to record the highest observed jacking speeds across
461 the various drives studied. The reduction of stresses acting on the pipe outer surface together
462 with the retention of lubricant resulted in relatively low jacking forces. This resulted in an
463 average measured jacking force of only 4.8 kN/m, for which the back-analyzed μ_{avg} was 0.07,
464 significantly lower than the recommended value of 0.1 by Stein et al. (1989).

465 For Drive D (shale), the calculated σ_{EV} value of 11.7 kN/m² indicated that arching effect
466 was reduced, similar to Drive B. Similarly to Drive B, the volume of injected lubricant was

467 well in excess of the theoretical overcut volume. It was likely that much of the injected
468 lubrication was lost into the surrounding geology through fissures. However, Drive D
469 encountered extended stoppage at the clay-shale interface, resulting in highly scattered
470 jacking forces in the shale section (see Fig. 3(d)).

471 These observations indicate that geology had a significant effect on the jacking forces due
472 to the stresses acting on the pipe by virtue of the arching effect. Subsequently, jacking forces
473 affected the response of the construction process, i.e. lubricant usage and jacking speeds. This
474 shows the coupling of arching and lubrication effects on jacking forces during pipe-jacking.
475 Therefore, it is summarized that:

- 476 (i) Sandstone (Drive A): Significant arching, relatively low jacking forces;
477 subsequently lower lubricant usage.
- 478 (ii) Phyllite (Drive C): Strongest arching due to folds and metamorphic nature, lowest
479 jacking forces; subsequently moderate lubricant usage.
- 480 (iii) Shale (Drive B & D): Reduced arching, relatively high jacking forces;
481 subsequently higher lubricant usage.

482 **Effect of geology on lubrication**

483 Drive A in sandstone had minimal lubrication, with only 47 L/m injected into the
484 theoretical overcut of 87 L/m as summarized in Table 4. However, the back-analyzed μ_{avg} of
485 0.31 still corresponded well with the recommended upper limit of 0.3 as recommended by
486 Stein et al. (1989) for lubricated drives. Drives B & C seem to be well-lubricated, as the
487 back-analyzed values of μ_{avg} were within the limits of 0.1 and 0.3 as recommended by Stein
488 et al. (1989) for lubricated pipe-jacking drives. For Drive B, the volume of injected lubricant
489 was 682 L/m, largely in excess of the theoretical overcut of 87 L/m (see Table 4). For Drive
490 C, the volume of injected lubricant amounted to 181 L/m, compared to the theoretical overcut
491 of 113 L/m. In both Drives B & C, the injected lubrication was in excess of the theoretical

492 overcut annulus, implying a continuous effort to saturate the overcut annulus. However, in
493 Drive B, it seems that there was significant loss of lubrication in order to sustain well-
494 lubricated conditions during pipe-jacking.

495 The excessive injection of lubricant observed in Drives B & D indicated a loss of
496 lubrication during the pipe-jacking works. This could imply difficulties in maintaining a
497 watertight overcut, most likely due to surrounding rock fissures or the inability of the
498 lubrication to form a filter cake of low permeability (Pipe Jacking Association, 1995).

499 A permeable overcut would mitigate the establishment of a discrete lubricating layer
500 between the pipe and the surrounding geology. Fig. 5(a) shows a schematic illustration of the
501 postulated lubrication scenario for Drives B & D. The lack of lubrication retained in the
502 overcut could also cause an increase in pipe-rock contact due to the loss of buoyant
503 lubricating forces acting on the pipe, that otherwise would have supported the pipe in fluid
504 suspension (French Society for Trenchless Technology, 2006; Pipe Jacking Association,
505 1995). Fig. 5(b) shows how buoyant forces can be achieved in a stable watertight bore, which
506 was the postulated situation for Drives A & C.

507 **Effect of stoppages on jacking forces**

508 Stoppages also had significant effects on jacking forces during tunneling through rock. In
509 Drive D, the initial transition from clay into rock corresponded with low jacking speeds of 3
510 mm/min (see Fig. S7), indicating difficulties in traversing through the change in geology.
511 This difficulty was reflected by the suspension of tunneling activities lasting 19 days. Upon
512 resumption of tunneling works, the average volume of injected lubricant increased from 380
513 L/m in clay to 729 L/m in rock, compared with a theoretical overcut volume of 113 L/m. For
514 the shale section, the average measured jacking force was 81.1 kN/m, with a computed σ_{EV} of
515 11.7 kN/m². The back-analyzed μ_{avg} of 0.71 easily exceeded the suggested values for
516 lubricated drives. It is also noted that the jacking forces in this shale section of Drive D

517 fluctuated greatly. The line of best fit depicting the average measured jacking force was
518 accurate to only $R^2 = 0.45$. Restarting of jacking works after extended stoppages produce
519 large static frictional resistance (Chapman and Ichioka, 1999; Norris, 1992; Sofianos et al.,
520 2004). The fluctuation of jacking forces seemed to have resulted from the restarting of works.
521 Additionally, stoppages can significantly impact lubricant use, particularly when pipe-jacking
522 through fissured geology. Any lubricant present in the overcut would be lost into fissures,
523 which act as drains. Upon resumption of pipe-jacking, the void overcut would need to be
524 refilled with lubricant. Re-injection of lubrication is usually ineffective during a restart due to
525 squeezing of the soil and rock surrounding the pipeline. Ground squeezing reduces the
526 overcut area and increases pipe-rock contact area. Full lubrication of the overcut is able to
527 provide uplift and buoyancy to the pipeline, allowing for full suspension of the jacked pipes.
528 This results in reduced contact between the pipe and the surrounding geology, particularly at
529 the pipe invert.

530 **CONCLUSIONS**

531 Tunneling rock spoils collected from the decantation chambers of four different pipe-
532 jacking sites in Kuching City, Malaysia were tested for the assessment of physical
533 characteristics and geotechnical strength properties. The scalped test specimens were
534 classified as sand-sized and poorly-graded. Direct shear tests were conducted on these
535 scalped, reconstituted tunneling rock spoils in order to characterize them so that assessment
536 of pipe-jacking forces could be better understood and reliably estimated.

537 Results from the direct shear tests were then applied to a well-established jacking force
538 model and subsequently benchmarked against field measured jacking loads. The assessment
539 of jacking forces was conducted by considering the vertical stresses at the pipe crown, σ_{EV}
540 and the volumes of lubricant injected. The back-analyzed frictional coefficient values derived
541 from the four pipe-jacking drives in the Tuang Formation of Kuching City have been found

542 to be reliable and have been explained in relation to their surrounding geologies. The
543 consistencies in findings and discussions made herein are important for the reconstituted rock
544 spoils to be considered as friable, highly weathered ‘soft rock’, thus exhibiting characteristics
545 that tend towards soil behavior. This has allowed for assessment of pipe-jacking forces using
546 jacking force equations developed for pipe-jacking drives in soil. Water-tightness of the
547 overcut region has been found to be important in maintaining a discrete layer of lubrication
548 that can relieve frictional stresses along the pipe-rock interface. Comparison of the studied
549 drives has shown that arching effects, jacking forces, amount and pattern of lubricant use as
550 well as jacking speeds can be strongly related to the traversed geologies during pipe-jacking
551 works. Stoppages were observed to be a significant factor that can lead to higher jacking
552 forces upon resumption of a jacking drive. Although the assessment of jacking forces through
553 rocks is limited in existing jacking force models, the current study shows that back-analyzed
554 μ_{avg} can be used to evaluate pipe-jacking forces through weathered geology.

555 **ACKNOWLEDGMENT**

556 The Authors would like to express their thanks for the generosity shown by Hock Seng
557 Lee Bhd. and Jurutera Jasa (Sarawak) Sdn. Bhd. during this study. The authors are also
558 thankful to Ms. Hsiao-Yun Leong, Mr. Mohammud Irfaan Peerun, and Mr. Yi-Zhou Tan for
559 assisting in the work described in this paper.

560 **SUPPLEMENTAL DATA**

561 Figs. S1 to S10 are available online in the ASCE Library (www.ascelibrary.org).

562 **REFERENCES**

563 Anubhav, S., and Basudhar, P. K. (2013). “Interface behavior of woven geotextile with rounded and
564 angular particle sand.” *J. Mater. Civ. Eng.*, 25(12), 10.1061/(ASCE)MT.1943-5533.0000774.

565 Anyaegbunam, A. J. (2015). "Nonlinear power-type failure laws for geomaterials: synthesis from
566 triaxial data, properties, and applications." *Int. J. Geomech.*, 15(1), 04014036.

567 Arulrajah, A., Rahman, M. A., Piratheepan, J., Bo, M. W., and Imteaz, M. (2013). "Evaluation of
568 interface shear strength properties of geogrid-reinforced construction and demolition materials
569 using a modified large scale direct shear testing apparatus." *J. Mater. Civ. Eng.*, 26(5),
570 10.1061/(ASCE)MT.1943-5533.0000897.

571 American Society for Testing and Materials (ASTM). (2000), Standard Practice for Classification of
572 Soils for Engineering Purposes (Unified Soil Classification System), *ASTM-D2487-00*, West
573 Conshohocken, PA.

574 American Society for Testing and Materials (ASTM). (2002), Standard Test Method for Particle-Size
575 Analysis of Soils, *ASTM-D422-63*, West Conshohocken, PA.

576 American Society for Testing and Materials (ASTM). (2003), Standard Test Method for Direct Shear
577 Test of Soils under Consolidated Drained Conditions, *ASTM-D3080-03*, West Conshohocken, PA.

578 Barla, M., Camusso, M., and Aiassa, S. (2006). "Analysis of jacking forces during microtunnelling in
579 limestone." *Tunn. Undergr. Sp. Tech.*, 21(6), 668-83.

580 Bhasin, R., Barton, N., Grimstad, E., and Chryssanthakis, P. (1995). "Engineering geological
581 characterization of low strength anisotropic rocks in the Himalayan region for assessment of tunnel
582 support." *Eng. Geol.*, 40(3-4), 169-93.

583 Cerato, A. B., and Lutenecker, A. J. (2006). "Specimen size and scale effects of direct shear box tests
584 of sands." *Geotech. Test. J.*, 29(6), 507-16.

585 Chapman, D. N., and Ichioka, Y. (1999). "Prediction of jacking forces for microtunnelling
586 operations." *Tunn. Undergr. Sp. Tech.*, 14(1), 31-41.

587 Charles, J. A., and Watts, K. S. (1980). "The influence of confining pressure on the shear strength of
588 compacted rockfill." *Géotechnique*, 30(4), 353-67.

589 Choo, C. S., and Ong, D. E. L. (2012). "Back-analysis of frictional jacking forces based on shear box
590 testing of excavated spoils." *Proc., 2nd Int. Conf. on Geotechnique, Construction Materials and
591 Environment*, GEOMATE International Society, Tsu, Mie, Japan, pp. 462-7.

592 Collins, I. F., Gunn, C. I. M., Pender, M. J., and Yan, W. (1988). "Slope stability analyses for
593 materials with a non-linear failure envelope." *Int. J. Numer. Anal. Meth. Geomech.*, 12(5), 533-50.

594 De Mello, V. F. B. (1977). "Reflections on design decisions of practical significance to embankment
595 dams." *Géotechnique*, 27(3), 281-354.

596 Deere, D. U. 1989, *Rock quality designation (RQD) after twenty years*, U.S. Army Corps of Engineers
597 Contract Report GL-89-1, Waterways Experiment Station, Vicksburg, Mississippi.

598 Desai, C. S., and Salami, M. R. (1987). "Constitutive model for rocks." *J. Geotech. Engrg.*, 113(5),
599 10.1061/(ASCE)0733-9410(1987)113:5(407).

600 Drescher, A., and Christopoulos, C. (1988). "Limit analysis slope stability with nonlinear yield
601 condition." *Int. J. Numer. Anal. Meth. Geomech.*, 12(3), 341-5.

602 French Society for Trenchless Technology (2006). *Microtunneling and Horizontal Drilling :
603 Recommendations : French National Project "Microtunnels" : Recommendations*, ISTE Ltd,
604 London.

605 Gurocak, Z., Solanki, P., Alemdag, S., and Zaman, M. M. (2012). "New considerations for empirical
606 estimation of tensile strength of rocks." *Eng. Geol.*, 145-1461-8.

607 Head, K. H. (1992). *Manual of soil laboratory testing. Vol. 2, Permeability, shear strength and
608 compressibility tests*, Halsted Press, New York.

609 Iai, M., and Luna, R. (2011). "Direct shear tests on JSC-1A lunar regolith simulant." *J. Aerosp. Eng.*,
610 24(4), 10.1061/(ASCE)AS.1943-5525.0000082.

611 Jasinge, D., Ranjith, P. G., Choi, S. K., Kodikara, J., Arthur, M., and Li, H. (2009). "Mechanical
612 properties of reconstituted Australian black coal." *J. Geotech. Geoenviron. Eng.*, 135(7),
613 10.1061/(ASCE)GT.1943-5606.0000010.

614 Jewell, R. A. (1986). "Direct shear tests on sand." *Géotechnique*, 39(2), 309-22.

615 Lade, P. V. (2010). "The mechanics of surficial failure in soil slopes." *Eng. Geol.*, 114(1-2), 57-64.

616 Lade, P. V., Yamamuro, J. A., and Bopp, P. A. (1996). "Significance of particle crushing in granular
617 materials." *J. Geotech. Engrg.*, 122(4), 10.1061/(ASCE)0733-9410(1996)122:4(309).

618 Li, Y. R., and Aydin, A. (2010). "Behavior of rounded granular materials in direct shear: Mechanisms
619 and quantification of fluctuations." *Eng. Geol.*, 115(1-2), 96-104.

620 Norris, P. M. (1992). "The behaviour of jacked concrete pipes during site installation", PhD thesis,
621 Pembroke College, Oxford University, viewed 4 February 2010.

622 Ong, D. E. L., and Choo, C. S. (2011). "Sustainable construction of a bored pile foundation system in
623 erratic phyllite." *ASEAN Australian Engineering Congress*.

624 Osumi, T. (2000). "Calculating jacking forces for pipe jacking methods." *No-Dig International*
625 *Research*, (October, 2000), 40-2.

626 Pellet-Beaucour, A. L., and Kastner, R. (2002). "Experimental and analytical study of friction forces
627 during microtunneling operations." *Tunn. Undergr. Sp. Tech.*, 17(1), 83-97.

628 Pellet, F. L., and Keshavarz, M. (2014). "Shear behavior of the interface between drilling equipments
629 and shale rocks." *J Petrol Explor Prod Technol*, 4(3), 245-54.

630 Pipe Jacking Association (1995). *Guide to best practice for the installation of pipe jacks and*
631 *microtunnels*, 1st edn, Pipe Jacking Association, London, England.

632 Potyondy, J. G. (1961). "Skin friction between various soils and construction materials."
633 *Géotechnique*, 11(4), 339-53.

634 Ramamurthy, T., Rao, G. V., and Singh, J. (1993). "Engineering behaviour of phyllites." *Eng. Geol.*,
635 33(3), 209-25.

636 Saroglou, H., Marinos, P., and Tsiambaos, G. (2004). "The anisotropic nature of selected
637 metamorphic rocks from Greece." *J. S. Afr. Inst. Min. Metall.*, 104(4), 217-22.

638 Shea Jr, W. T., and Kronenberg, A. K. (1993). "Strength and anisotropy of foliated rocks with varied
639 mica contents." *J. Struct. Geol.*, 15(9-10), 1097-121.

640 Shou, K. J., Yen, J., and Liu, M. (2010). "On the frictional property of lubricants and its impact on
641 jacking force and soil-pipe interaction of pipe-jacking." *Tunn. Undergr. Sp. Tech.*, 25(4), 469-77.

642 Simoni, A., and Houlsby, G. T. (2006). "The direct shear strength and dilatancy of sand-gravel
643 mixtures." *Geotech. Geol. Eng.*, 24(3), 523-49.

644 Singh, M., Rao, K. S., and Ramamurthy, T. (2002). "Strength and deformational behaviour of a
645 jointed rock mass." *Rock Mech. Rock Eng.*, 35(1), 45-64.

646 Sofianos, A. I., Loukas, P., and Chantzakos, C. (2004). "Pipe jacking a sewer under Athens." *Tunn.*
647 *Undergr. Sp. Tech.*, 19(2), 193-203.

648 Soon, S. C., and Drescher, A. (2007). "Nonlinear failure criterion and passive thrust on retaining
649 walls." *Int. J. Geomech.*, 7(4), 318-22.

650 Staheli, K. (2006). "Jacking force prediction an interface friction approach based on pipe surface
651 roughness", PhD thesis, Georgia Institute of Technology, viewed 29 January 2010.

652 Standards Australia. (1993), Geotechnical site investigations, *AS 1726-1993*, Australia.

653 Standards Australia. (1998), Soil strength and consolidation tests - Determination of the shear strength
654 of a soil - Direct shear test using a shear box, *AS 1289.6.2.2-1998*, Australia.

655 Stein, D., Möllers, K., and Bielecki, R. (1989). *Microtunnelling : Installation and Renewal of*
656 *Nonman-Size Supply and Sewage Lines by the Trenchless Construction Method*, Ernst, Berlin,
657 Germany.

658 Tan, D. N. K. (1993). *Geology of the Kuching Area, West Sarawak, Malaysia*, Geological Survey of
659 Malaysia, Kuching, Malaysia.

660 Terzaghi, K. (1936). "Stress distribution in dry and in saturated sand above a yielding trap-door."
661 *Proc., 1st Intl. Conf. on Soil Mechanics and Foundation Engineering*, pp. 307-11.

662 Terzaghi, K. (1943). *Theoretical soil mechanics*, John Wiley & Sons, Inc.

663 Tiwari, R. P., and Rao, K. S. (2007). "Response of an anisotropic rock mass under polyaxial stress
664 state." *J. Mater. Civ. Eng.*, 19(5), 10.1061/(ASCE)0899-1561(2007)19:5(393).

665 Wang, J. J., Zhang, H. P., Tang, S. C., and Liang, Y. (2013). "Effects of particle size distribution on
666 shear strength of accumulation soil." *J. Geotech. Geoenviron. Eng.*, 139(11),
667 10.1061/(ASCE)GT.1943-5606.0000931.

668 Yang, X. L., and Yin, J. H. (2004). "Slope stability analysis with nonlinear failure criterion." *J. Eng.*
669 *Mech.*, 130(3), 10.1061/(ASCE)0733-9399(2004)130:3(267).

670 Yilmaz, I. (2009). "A new testing method for indirect determination of the unconfined compressive
671 strength of rocks." *Int. J. Rock Mech. Min.*, 46(8), 1349-57.

672 Yu, X., Ji, S., and Janoyan, K. D. (2006). "Direct shear testing of rockfill material." *GeoShanghai*
673 *2006*, American Society of Civil Engineers, Reston, Virginia, pp. 149-55.

Table 1. Physical properties of scalped tunneling rock spoils.

Test no. / Drive	Test 1 / Drive A	Test 2 / Drive B	Test 3 / Drive C	Test 4 / Drive D
Geology	Sandstone	Shale	Phyllite	Shale
D_{60} (mm)	0.53	0.51	0.73	0.73
D_{30} (mm)	0.25	0.35	0.29	0.27
D_{10} (mm)	0.11	0.21	0.10	0.13
D_{50} (mm)	0.45	0.45	0.55	0.61
Weighted average particle size, D_{av} (mm)	1.02	0.59	0.80	0.82
Coefficient of uniformity, C_u	3.53	2.32	5.57	5.20
Coefficient of curvature, C_c	0.77	1.16	1.12	0.67
Material classification	Poorly graded sand-sized spoils (SP)	Poorly graded sand-sized spoils (SP)	Poorly graded sand-sized spoils (SP)	Poorly graded sand-sized spoils (SP)
Applied effective normal stresses for direct shear tests (kPa)	25, 50, 75, 100 255, 600	50, 100, 250, 400	100, 250, 380, 400	150, 375, 395, 500
Densities of tested samples (kN/m^3)	15.9 – 16.9	13.7 – 14.8	– ^a	15.5 – 16.7

^aNote: Measurements were not made for Test 3 specimens.

Table 2. Shear strength of tunneling rock spoils and rockfill materials using power law

functions, where $\tau = A \cdot (\sigma')^B$

Material type	Geology	A	B	Source
Tunneling rock spoils	Sandstone (Test 1 – peak)	4.68	0.76	This study
	Sandstone (Test 1 – residual)	2.24	0.84	
	Phyllite (Test 3 – peak)	1.92	0.87	
	Phyllite (Test 3 – residual)	1.07	0.96	
	Shale (Test 4 – peak)	3.86	0.79	
	Shale (Test 4 – residual)	3.37	0.78	
Rockfill	Sandstone	6.8	0.67	Charles and Watts (1980)
	Slate	5.3	0.75	
	Slate	3.0	0.77	
	Basalt	4.4	0.81	
	Basalt	1.54	0.821	De Mello (1977)
	Diorite	1.10	0.870	
	Conglomerate	1.27	0.846	
	Conglomerate	1.19	0.881	
	Conglomerate	1.59	0.808	

Table 3. Parameters used in pipe-jacking force model for back-analyses of μ_{avg}

Drive (Test no.)		Drive A (Test 1)	Drive B (Test 2)	Drive C (Test 3)	Drive D (Test 4)
Geology		Sandstone	Shale	Phyllite	Shale
D_e (m)		1.43	1.43	1.78	1.78
γ (kN/m ³)		22	22	22	22
h (m)		12.5	12.5	18.5	19.5
Power function, $\tau = A \cdot (\sigma')^B$ applied to data points ^a	A_p	4.68	N/A since power function is not applicable. ^b	3.86	1.92
	B_p	0.76		0.79	0.87
	A_r	2.24		3.37	1.07
	B_r	0.84		0.78	0.96
MC parameters ^a	c'_p (kPa)	50.8	0	57.8	29.0
	ϕ'_p (°)	47.8	41.4	44.3	38.7
	c'_r (kPa)	24.2	0	50.3	8.3
	ϕ'_r (°)	39.6	37.6	39.2	39.4
Average measured jacking forces (kN/m)		14.4	29.0	4.8	81.1
Back-analyzed μ_{avg} , using Eq. (1)		0.31	0.20	0.07	0.71
R^2		0.93	0.90	0.78	0.45

^aNote: Subscript p denotes peak values; subscript r denotes residual values

^bNote: Data points can be conveniently represented by line of best fit, hence power law is not necessary here.

Table 4. Comparison of pipe-jacking performance for various drives

Test no. Drive Geology	1 Drive A Sandstone	2 Drive B Shale	3 Drive C Phyllite	4 Drive D Shale
Length of nearby rock cores extracted (m)	4.5	5.1	15.1	6.0
Average RQD (%)	0	26.0	17.5	14.0
Length of rock cores with RQD = 0 (m)	4.5	0.65	7.6	0.7
Average volume of lubricant injected including losses (L/m)	47	682	181	729
Average theoretical overcut volume (L/m)	87	87	113	113
Effective overburden pressure (without arching) (kN/m ²)	150	150	222	234
Average jacking speed (mm/min)	16	10	44	34
Average measured face support pressure (kN/m ²)	104	68	47	115
Cutter face diameter (m)	1.47	1.47	1.82	1.82
TBM weight (tonnes)	15	15	20	20
Pipe weight (kN/m)	17.3	17.3	11.6	11.6
Calculated σ_{EV} (kN/m ²) (Eq. (2))	-20.8 ^a	34.1	-22.3 ^a	11.7
Average measured jacking forces (kN/m)	14.4	29.0	4.8	81.1
Back-analyzed μ_{avg}	0.31	0.20	0.07	0.71

^aNote: Negative values of σ_{EV} (Eq. (2)) indicate possible presence of significant arching. For back-analysis of μ_{avg} , these negative values of σ_{EV}

were adjusted to be equal to zero (Terzaghi, 1943).

Figure 1

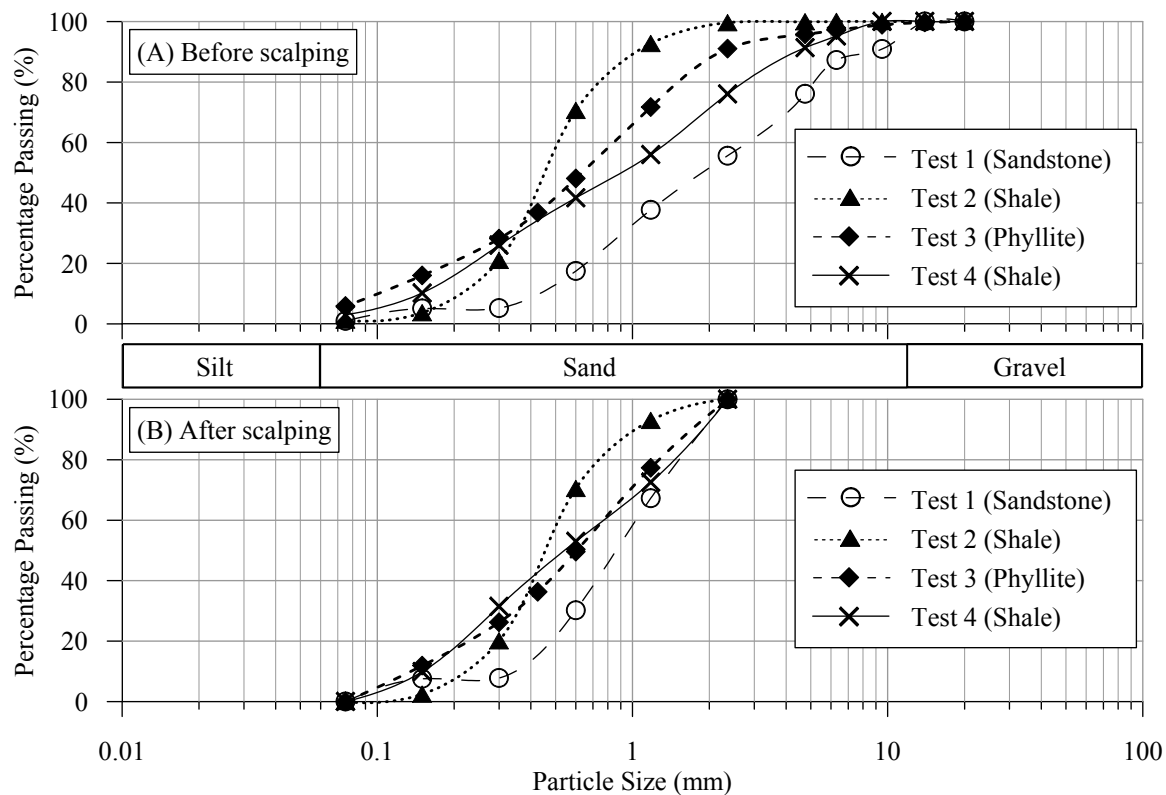


Figure 2

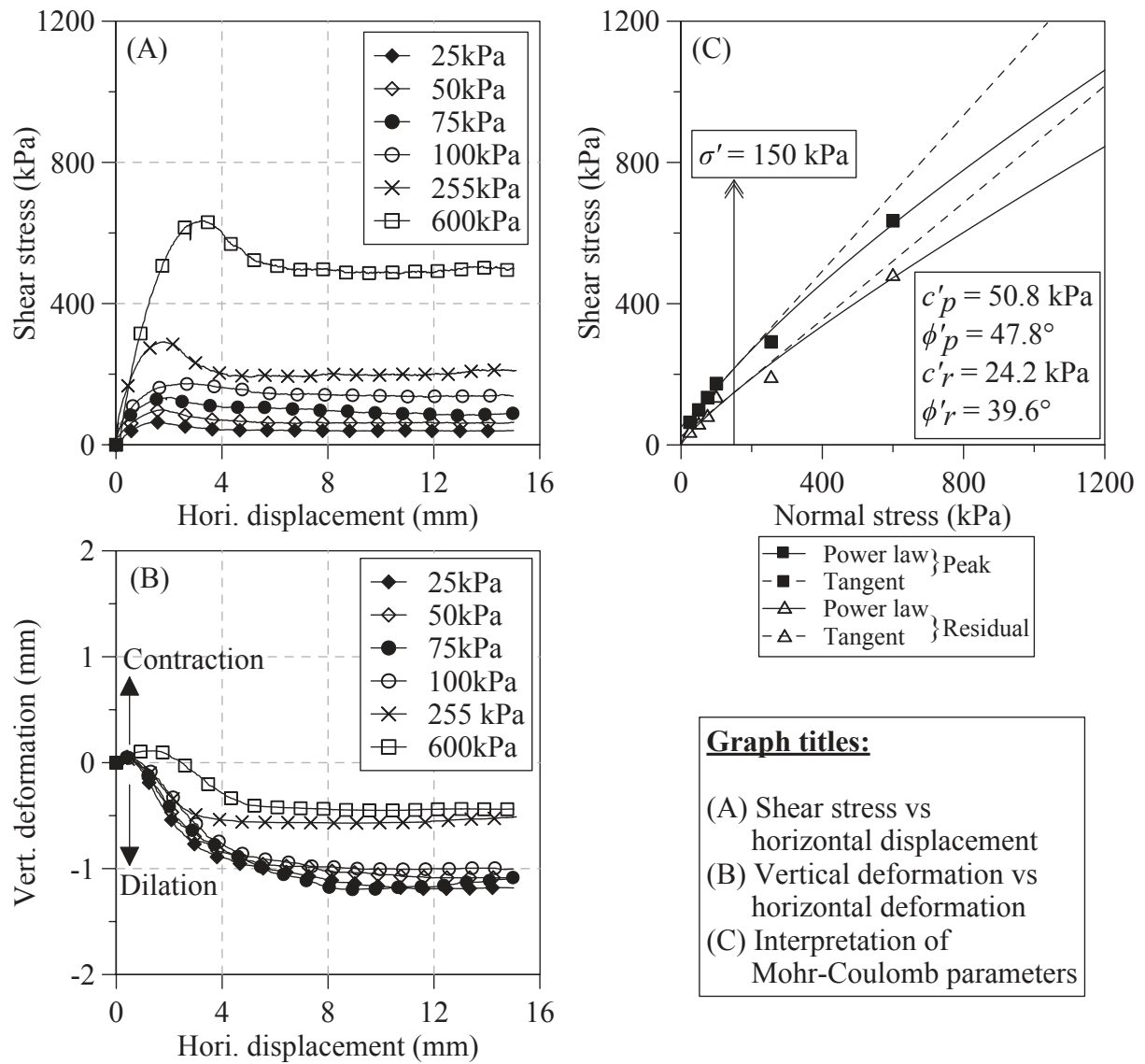


Figure 3

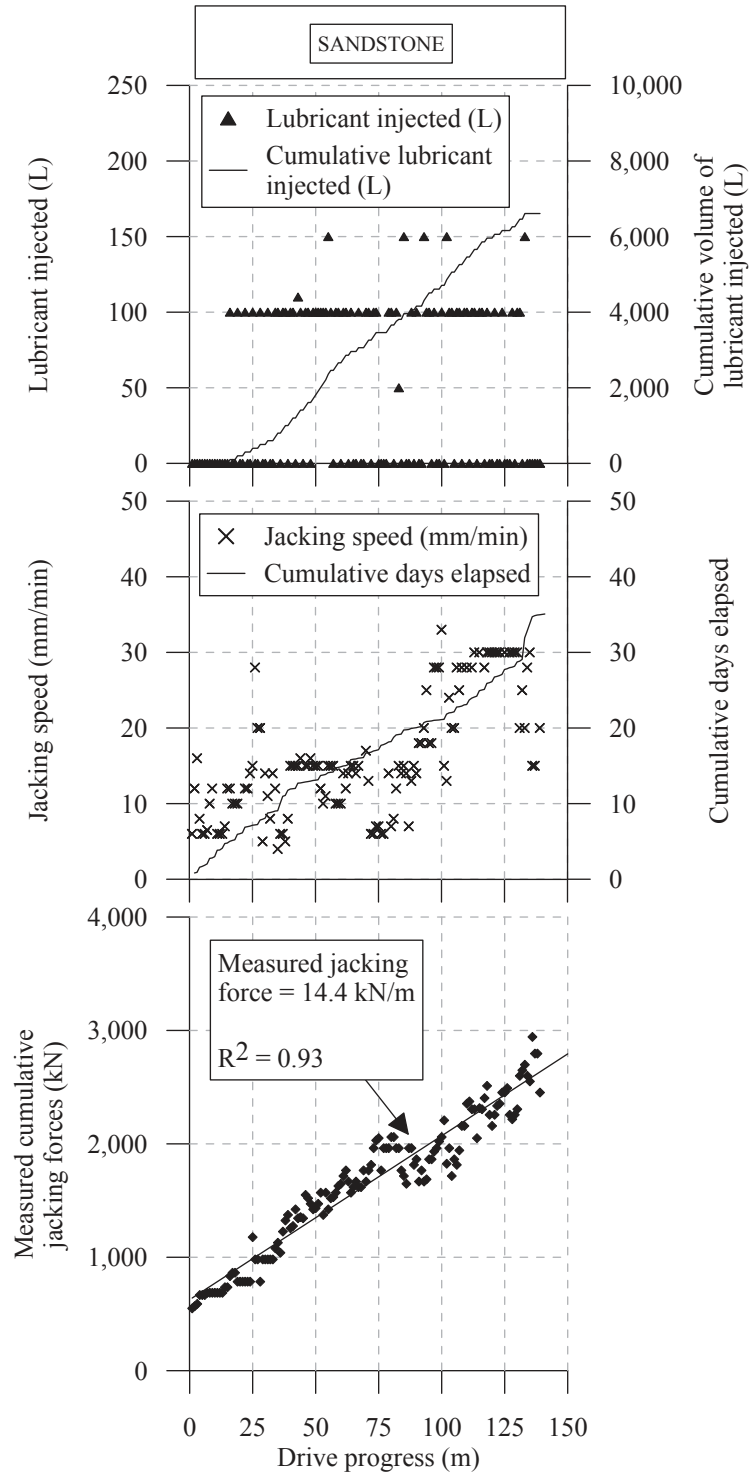


Figure 4

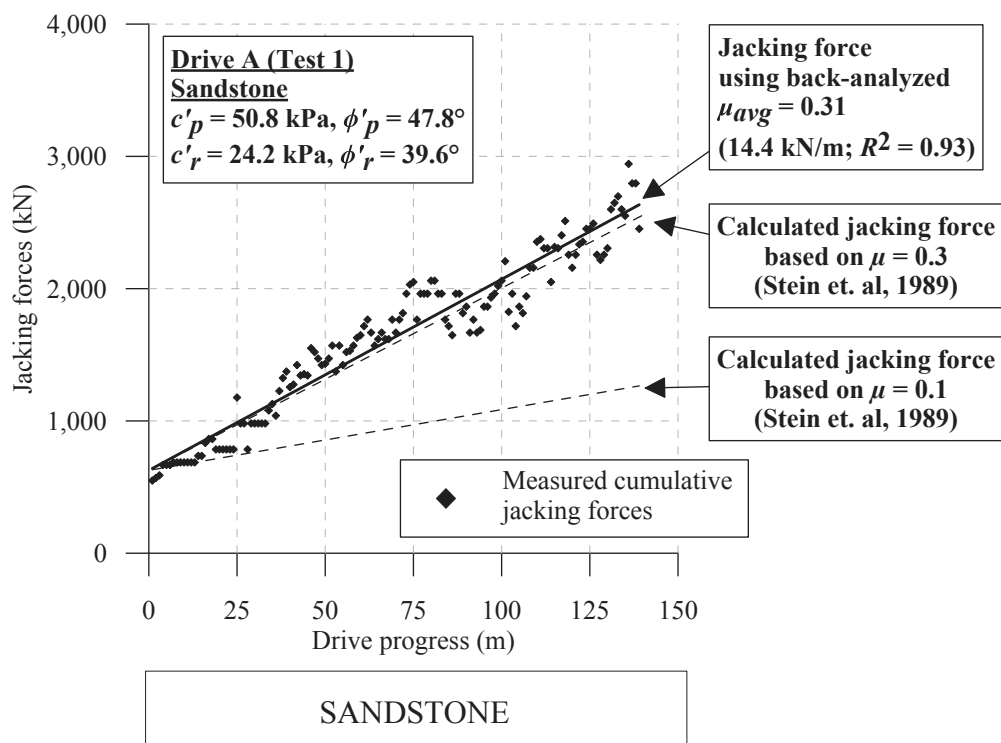
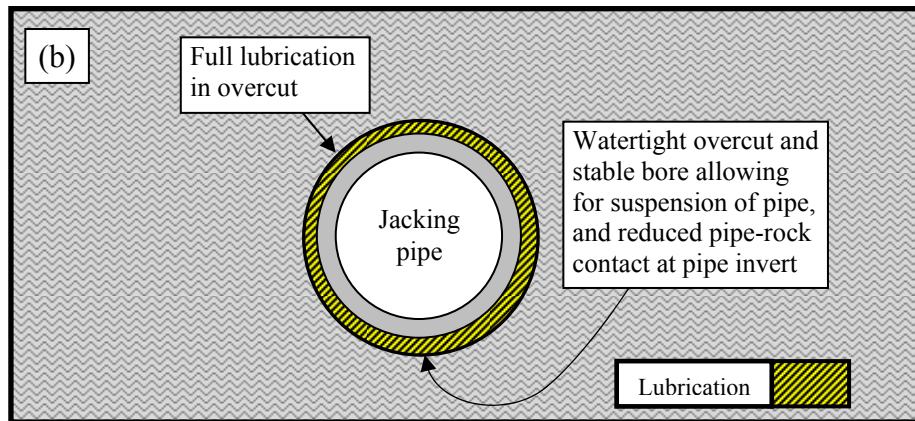
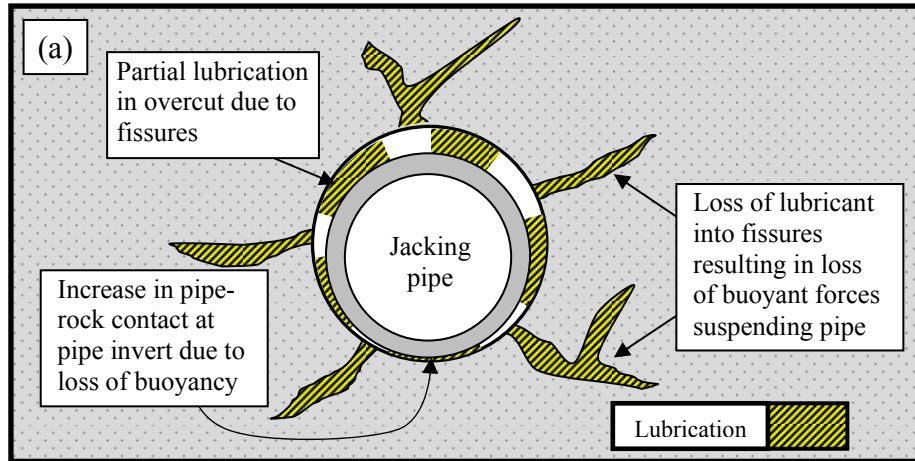


Figure 5



LIST OF TABLES

Table 1. Physical properties of scalped tunneling rock spoils.

Table 2. Shear strength of tunneling rock spoils and rockfill materials using power law functions, where

Table 3. Parameters used in pipe-jacking force model for back-analyses of μ_{avg}

Table 4. Comparison of pipe-jacking performance for various drives

LIST OF FIGURES

- Fig. 1. Particle size distribution of tunneling rock spoils; (A) before scalping; (B) after scalping to create a direct shear specimen
- Fig. 2. Results from direct shear testing of scalped tunneling rock spoils (Test 1)
- Fig. 3. Variations in measured jacking forces, jacking speed and volume of injected lubricant for the studied drives (Drive A)
- Fig. 4. Drive A (sandstone): Outcome of back-analyzed μ_{avg} in comparison to recommended upper & lower bounds
- Fig. 5. Schematic diagrams showing pipe behavior under different degrees of lubricant retention in tunnel overcut in varying geological conditions; (a) partial loss of lubricant into rock fissures; (b) minimal loss of lubricant in a 'watertight' rock mass